

# CoCoNET: Co-Optimizing Computation and Communication for Distributed Machine Learning

Abhinav Jangda  
University of Massachusetts Amherst  
United States

Jun Huang  
Microsoft Research  
China

Guodong Liu  
Chinese Academy of Sciences  
China

Amir Hossein Nodehi Sabet  
University of California, Riverside  
United States

Madanlal Musuvathi  
Microsoft Research  
United States

Olli Sarikivi  
Microsoft Research  
United States

Todd Mytkowicz  
Microsoft Research  
United States

Youshan Miao  
Microsoft Research  
China

## Abstract

Modern deep learning workloads run on distributed hardware and are difficult to optimize — data, model, and pipeline parallelism require a developer to thoughtfully restructure their workload around optimized computation and communication kernels in libraries such as cuBLAS and NCCL.

The logical separation between computation and communication leaves performance on the table with missed optimization opportunities across abstraction boundaries. To explore these opportunities, this paper presents CoCoNET, which consists of a *compute language* to express programs with both computation and communication, a *scheduling language* to apply transformations on such programs, and a *compiler* to generate high performance kernels. Providing both computation and communication as first class constructs enables new optimizations, such as overlapping or fusion of communication with computation.

CoCoNET allowed us to optimize several data, model and pipeline parallel workloads in existing deep learning systems with very few lines of code. We show significant improvements after integrating novel CoCoNET generated kernels.

### ACM Reference Format:

Abhinav Jangda, Jun Huang, Guodong Liu, Amir Hossein Nodehi Sabet, Madanlal Musuvathi, Olli Sarikivi, Todd Mytkowicz, and Youshan Miao. 2022. CoCoNET: Co-Optimizing Computation and Communication for Distributed Machine Learning. In *Proceedings of ACM Conference (Conference'17)*. ACM, New York, NY, USA, 14 pages. <https://doi.org/10.1145/nnnnnnnn.nnnnnnn>

## 1 Introduction

The recent trend in machine learning towards larger models is far from over — from BERT [9] at 340 million and GPT-2 [34] at 8.3 billion parameters, the GPT-3 model now sports 175 billion parameters. As these models exceed the memory capacities of a single GPU, training these models requires distributing the computation through a combination of data parallelism [19], model parallelism [6], and pipeline parallelism [14, 24, 25].

Distributed deep learning workloads today involve highly optimized computation kernels communicating through well-established MPI abstractions such as AllReduce. For instance, NCCL [29], a communication kernel library from NVIDIA, provides manually optimized implementations of different MPI primitives, and users are required to structure their computations around these primitives. A key hypothesis of this paper is that as machine learning workloads become distributed, the performance of these communication kernels will become the primary scalability bottleneck. As such, maximizing performance and scalability will require us to break the current abstraction boundary and use custom communication kernels.

To this effect, we propose the CoCoNET<sup>1</sup> for generating highly-optimized custom communication kernels. Figure 1 presents the overview of CoCoNET. CoCoNET includes a DSL to express programs containing both computation and collective communication primitives. Inspired by Halide [30], CoCoNET includes a *scheduling language* to specify an execution schedule of the program using a set of transformations. These transformations can be used to optimize a program by breaking the communication and computation boundary. CoCoNET's *code generator* automatically generates high-performance computation and communication kernels from a program and its schedule.

Using a set of semantic preserving transformations, CoCoNET allows users to quickly apply various optimizations to generate optimized implementations for specific hardware, topology, model sizes, and data sizes. Unlike existing techniques for optimizing distributed machine learning, such as GShard [20], PyTorch's DDP [21], and DSLs for optimizing stencil computations [8, 12, 13, 30, 35], CoCoNET provides communication collectives as constructs in the language, which allows new optimizations, such as topology aware

<sup>1</sup>CoCoNET stands for "Communication and Computation optimization for neural Networks. We will make our implementation publicly available.

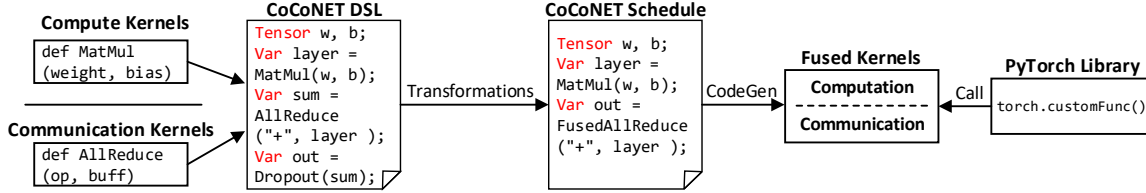


**Figure 1.** Overview of CoCoNET’s workflow. First, a user expresses a deep learning algorithm in the DSL to create a program containing both computation (MatMul) and communication (AllReduce). Then, the user applies several transformations to optimize the program while keeping the algorithm unchanged, such as fusing AllReduce and Dropout into FusedAllReduce. Finally, CoCoNET generates custom communication and computation code, which is available through PyTorch.

overlap of computation and communication, and fused communication with computation. Similar to [31], CoCoNET’s optimizations can decrease memory usage per GPU to allow larger batch sizes, thereby, decreasing training time.

We use CoCoNET to optimize data parallel training, model parallel inference, and pipeline parallel inference. Using CoCoNET we generated optimized kernels for the Adam [17] and LAMB [38] parameter update, which outperforms hand-written versions from NVIDIA’s Apex [28] library by upto 2×. These kernels were written in less than 20 lines of code(LoC), while their hand-written Apex versions were written in 6.2K LoC and ZeRO [31] version in 3K LoC. We optimized model parallel implementations of Megatron-LM [34] using CoCoNET in 10 lines of code by using CoCoNET’s overlap of communication and computation to obtain 1.4× speedup over Megatron-LM. Finally, we improved inference in pipeline parallelism of Megatron-LM using CoCoNET’s overlap approach of different communication operations to achieve 1.19× speedup over baseline Megatron-LM.

## 2 CoCoNET DSL

CoCoNET extends data representation in existing deep learning and allows expressing both computation and communication in its domain specific language. Unifying the expression of computation and communication for distributed deep learning in the same DSL is the foundation to enable optimizations across computation and communication.

### 2.1 Tensor Layout

CoCoNET extends existing concept of tensor in deep learning frameworks from single device data into distributed forms. Apart from item datatype (INT32, FP16) and shape which are already defined in a traditional tensor, a CoCoNET tensor extends with description of how it is distributed across a set of ranks. We follow MPI [10] terminology RANK to represent the process ID of a distributed process and the set of all processes within the same communication group as WORLD. CoCoNET supports dividing consecutive ranks into one or more groups. RANK and GROUP denote the rank and group of current process, respectively. Similar to MPI, CoCoNET follows a single program multiple data (SPMD) parallelism where each rank runs the same pattern but with different ID.

```

1 Tensor w(FP16, [H,H], Sliced(0), WORLD, RANK);
2 Tensor b(FP16, [H], Replicated, WORLD);
3 Tensor in(FP16, [B,S,H], Sliced(2), WORLD, RANK);
4 Tensor r(FP16, [B,S,H], Replicated, WORLD);
5
6 // layer(FP16, [B,S,H], Local, WORLD, RANK)
7 Var layer = MatMul(in, w);
8 // sum(FP16, [B,S,H], Replicated, WORLD)
9 Var sum = AllReduce("+", layer);
10 // dropout(FP16, [B,S,H], Replicated, WORLD)
11 Var dropout = Dropout(sum + b, 0.1);
12 // out(FP16, [B,S,H], Replicated, WORLD)
13 Var out = dropout + r;
14
15 Execute self_attention({w,in,b,r}, {out});

```

**Figure 2.** An example program in CoCoNET. (B: batch size, S: sequence length, H: hidden dimension size)

CoCoNET includes three distributed layouts: *sliced*, *replicated*, and *Local*. A *sliced* tensor represents one that is equally distributed to all the nodes in a group along specified dimension with RANK identifying the slice. For example, in Figure 2, *w* is sliced among all ranks in WORLD in the first dimension and *in* is sliced in the third dimension. A tensor can also be *replicated* across all ranks in a group where it has the same value on each rank and hence, it does not have a rank identifier. For example the model parameter *b* and the residual connection *r* are replicated as shown in Figure 2. A *local* tensor is one that has equal shape on all ranks but with different values on different ranks. Unlike replicated, local requires a RANK to identify the values. For example, in Figure 2, *layer* is a local tensor that represents the partial result of a matrix multiplication (MatMul) operation. A Scalar is a zero-dimensional Tensor that represents a variable available on all ranks. We will discuss shape and distributed property tags of intermediate tensors in the next section.

### 2.2 CoCoNET’s Operations

CoCoNET programs inherit the concept of data-flow graph (DFG) from existing deep learning frameworks, with operations as vertices and data dependencies as edges. Moreover, each tensor has the update function that reflects the new values of tensor in that position in DFG.

CoCoNET operations include local computations and cross rank communications on tensors. This includes collective communications such as AllReduce and AllGather, and P2P communications like Send and Recv. CoCoNET’s local computation operations can be mapped to existing neural networks operations, such as *dropout* and *matrix multiplication*. A Var represents the intermediate values obtained after performing an operation.

For instance, Figure 2 describes the Megatron-LM [34] model parallel logic on part of Self-Attention layer in CoCoNET. In this model parallel example, the linear layer’s weight ( $w$ ) and the input ( $in$ ) are sliced across all ranks while the bias ( $b$ ) and residual ( $r$ ) are replicated on all ranks. CoCoNET requires the inputs to have the shape and distribution property tags. However, a Var’s shape and property is implied by the operation. For example, Line 7 performs a MatMul operation on the input and the weights of the linear layer. Note that in this MatMul the summation dimension is the sliced H dimensions of  $in$  and  $w$  which disappear in the output layer. Therefore, layer represent a partial result of the MatMul operation and the shape and distribution property of it are  $[B, S, H]$  and Local, respectively. This is followed by an AllReduce in Line 9 to compute the sum of layer. This makes the Local property of layer a replicated property in sum as an AllReduce has the same output on all ranks. Lines 11–13 perform pointwise computations that involves adding the bias, using dropout as the activation and adding the residual of previous layer. The shape and distribution property of these operations are the same as sum. Finally, an Execute defines the inputs and outputs of the program.

### 2.3 Fused Communication Collectives

To enable efficient computations on the output of communication, CoCoNET contains fused communication collectives as primitives. Due to the separation of communication and computation in existing deep learning frameworks, communication collectives store their output from register to memory and then the upcoming computation reload the same data to register. Instead, fused communication collectives in CoCoNET skips the load-after-save between communication and computation by passing each element of the communication collective’s output through registers to the computation, thereby avoiding unnecessary memory accesses.

CoCoNET extends all common collective communication to fused communication collectives, such as FusedAllReduce and FusedReduceScatter. Each fused collective takes an extra computation operation (comp) and fuses the computation in the code, which is the earliest place when each element of output of collective communication is produced. For example, AllReduce implementations stores each element of output tensor in a register before writing it to the memory. When an element of the output tensor is in a register after reducing input elements of all ranks, the computation described by comp is performed on the value stored in that register.

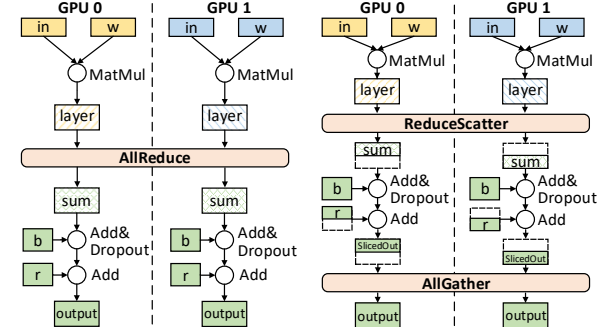


Figure 3. Equivalent programs (from Figure 2) using AllReduce (on left) or using ReduceScatter + AllGather (on right).

### 2.4 Overlapping Operations

CoCoNET supports overlapping two or more operations using its Overlap primitive. A common example for this construct is to overlap communication with the computation producing input of the collective. Overlapping consecutive communication primitives is another example where Overlap construct is applied with CoCoNET. Note that Overlap construct can only be used to overlap operations where one’s output is consumed immediately by another one and at least one of them is a communication kernel.

### 2.5 Equivalent Programs using Transformations

The way to express the same algorithm in CoCoNET DSL is not unique. For example, as shown in Figure 3, existing works [16, 20, 31] distributes the computation by first doing ReduceScatter to divide the summed values among all rank, then perform computation on the divided tensor, and finally performs AllGather to share the output of computation. Next section describes several output-invariant transformation between different concrete programs.

## 3 Schedules in CoCoNET

CoCoNET provides five categories of transformations to generate different schedules from the same program. Each transformation generates a new schedule by replacing source operations with target operations, while keep the program output unchanged. To ensure the dependencies in the DFG, each transformation is valid if and only if there is no cycle in the DFG after the transformation. CoCoNET automatically performs this check. We now present each transformation by applying them on the example program from Figure 2.

### 3.1 Fusing Operations

CoCoNET provides the fuse transformations to fuse two or more source operations into a single target operation based on one of the following policies. CoCoNET lowers each operation to a CUDA kernel and thus, fuse lets a developer control kernel invocations through fusion.

ALLREDUCE FUSE RS-AG: transforms consecutive ReduceScatter and AllGather into a single AllReduce.

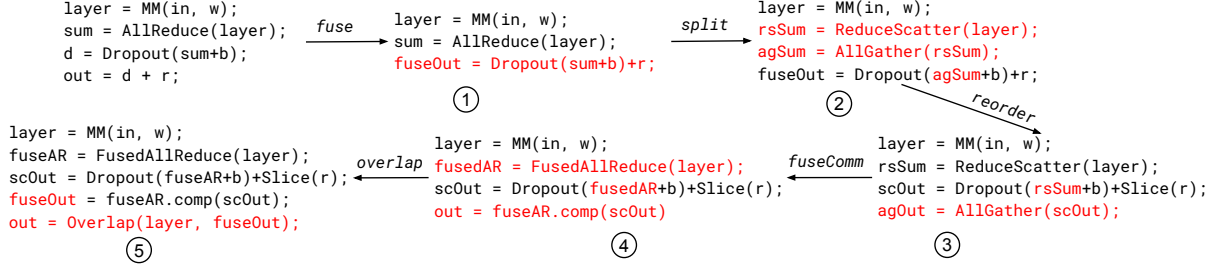


**Figure 4.** Different schedules produced by performing transformations on parallel program from Figure 2. Each schedule can be represented as a standalone CoCoNET program. Lines in red highlights the changes on this step.

ALLREDUCE FUSE B-R: transforms consecutive Reduce and Broadcast into a single AllReduce.

COMPUTE FUSE: fuses multiple computations into a single equivalent computation.

**Running Example** We fuse all pointwise computations in Figure 2, into a single computation.

```
fuseOut = fuse(d, out, ComputeFuse);
```

Figure 4 shows the equivalent CoCoNET implementation of this schedule in ①. The fuseOut operation performs both dropout and the residual addition in a single kernel and thus avoids redundant memory accesses.

### 3.2 Splitting Operations

CoCoNET’s split transformation breaks a communication collective into two collectives based on two split policies:

ALLREDUCE SPLIT RS-AG splits an AllReduce into ReduceScatter to produce sliced tensors and all AllGather on the sliced tensors to obtain a replicated tensor.

ALLREDUCE SPLIT B-R splits an AllReduce into Reduce to produce a tensor on one of the ranks in WORLD and then Broadcast this tensor to all ranks in WORLD.

**Running Example** We split the AllReduce in Figure 2 into rsSum and agSum, where the former does a ReduceScatter on layer and the later does an AllGather on rsSum.

```
(rsSum, agSum) = split(layer, AllReduceSplitRSAG);
```

Figure 4 shows the equivalent CoCoNET implementation of this schedule in ②, where the input to fuseOut is replaced by agSum, which is the output of AllGather. In next section, we demonstrate how to swap the AllGather with the computation to perform slice computations.

### 3.3 Reordering Computation and Communication

CoCoNET provides reorder transformation that takes two source operations  $s_1$  and  $s_2$ , and based on the following policies returns two or more target operations  $t_1, t_2, \dots$

BROADCAST REORDER: reorders Broadcast with computation. Suppose  $s_1 = Broadcast(x, r)$  and  $s_2$  is computation, then  $t_1$  is the same computation as  $s_2$  but with two differences: (i) the tensors input to  $s_2$  are loaded from rank  $r$  because

input of Broadcast is local to  $r$ , and (ii)  $t_1$  replaces the use of  $s_1$  with  $x$ . Further,  $t_2$  performs Broadcast of  $t_1$  from rank  $r$ .

ALLGATHER REORDER: reorders AllGather with computation. Suppose  $s_1 = AllGather(x)$  and  $s_2$  is computation, then  $t_1$  is the same computation as  $s_2$  but with two differences: (i)  $t_1$  contains slices of all tensors input to  $t_2$  because AllGather takes a sliced tensor as input and (ii)  $t_1$  replaces the use of  $s_1$  with  $x$ . Moreover,  $t_2$  is changed to  $AllGather(t_1)$ .

If  $t_2$  is a fused computation, then AllGather or Broadcast is done on the outputs of these computations and output of program. Extra operations:  $t_3, t_4, \dots$ , denotes these AllGather or Broadcast. With further transformations, such as, asSlice which changes the layout of tensors input to program to slice, these extra operations are not needed. The dead function can be used to eliminate an inessential AllGather.

**Running Example** From the previous schedule, we reorder agSum, which does an AllGather on layer output with fuseOut to obtain: (i) scOut, which performs sliced computations, and (ii) agOut, which gathers the result of computation.

```
(scOut, agOut) = reorder(agSum, fuseComp, AllGatherReorder);
```

Figure 4 shows the equivalent CoCoNET program of this schedule in ③, where the input to Dropout is now the output of ReduceScatter, i.e., rsSum and computations are performed on slice of residual ( $r$ ) to produce a sliced output. Finally, AllGather collects the sliced output to obtain a replicated output. The next section demonstrates how to fuse both ReduceScatter and AllGather with the computation.

### 3.4 Fusing Computation and Communication

CoCoNET provides fusedComm transformation to fuse communication and computation into a single operation that performs fused communication collectives. We explain this transformation for FusedAllReduce, which is performed when FusedAllReduce is passed to fusedComm but this transformation can be easily generalized to other fused communication collectives. In this case the transformation is valid only when source operations performs ReduceScatter, sliced computation on the output of ReduceScatter, and AllGather



```

1 Var avg = AllReduce("+", g);
2 Var m_ = m.update(m*beta1+(1-beta1)*avg);
3 Var v_ = v.update(v*beta2+(1-beta1)*avg*avg);
4 Var m1 = m_/(1-beta1); v1 = v_/(1-beta2);
5 Var diff = lr * m1/(sqrt(v1));
6 Var p_ = p.update(p - diff);
7
8 Execute adam({g,p,v,m,lr}, {p_});

```

(a) Traditional implementation where tensors  $g$  is local to each rank and  $p, m$ , and  $v$  are replicated on all ranks.

```

1 fusedComp = fuse(m_, v_, m1, v1, p_);
2 (rsG, agG) = split(avg, AllReduceSplit1);
3 (scComp, agP, agM, agV) = reorder(agG, fusedComp,
4                               AllGatherReorder);
5 asSlice(m); asSlice(v); dead(agM); dead(agV);
6 fuseAR = fuseComm(rsG, scComp, agP,
7                 FusedAllReduce);

```

(b) An Optimized Schedule. Tensors  $g$  is local,  $p$  is replicated on all ranks, while  $m$  and  $v$  are sliced among all ranks.

**Figure 5.** Optimizing the parameter update using Adam in CoCoNET. The implementation takes four input tensors: (i) model parameters ( $p$ ), (ii) gradient of parameters ( $g$ ), and optimizer states, (iii) momentum ( $m$ ), and (iv) velocity ( $v$ ).

on the output of the computation. The target operation is a FusedAllReduce that performs all these operations.

**Running Example** From the previous schedule, we fuse operations in a single FusedAllReduce that generates a single kernel for communication and computations.

```

fuseAR = fuseComm(rsSum, scOut, agOut,
                 FusedAllReduce);

```

Figure 4 shows the equivalent implementation of this schedule in ④, where FusedAllReduce is used instead of AllReduce. The comp method of fusedAR specifies the computation to be fused with FusedAllReduce and returned out is the output.

### 3.5 Overlapping Computation and Communication

CoCoNET provides overlap transformation to overlap a series of producer-consumer operations. This transformation can be used to overlap communication operations or a computation with communication in distributed machine learning workloads. It takes two or more operations as input and returns a single operation.

**Running Example** We overlap the matrix multiplication with FusedAllReduce.

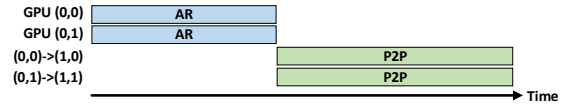
```

layerWithAR = overlap(layer, fusedAR);

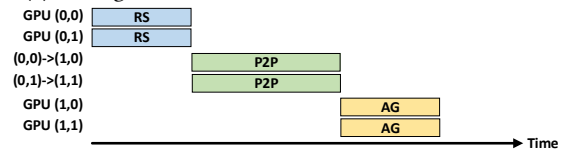
```

Figure 4 shows the equivalent implementation of this schedule in ⑤, where layer and fuseOut are overlapped.

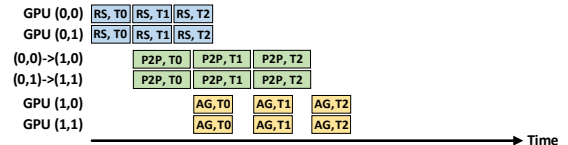
## 4 Optimizing Workloads with CoCoNET



(a) In Megatron-LM each GPU sends redundant data.



(b) After splitting AllReduce into ReduceScatter + AllGather, each GPU can send only a slice of data.



(c) Communication operations can be overlapped at the granularity of each *communication buffer tile* of data in single kernel call.

**Figure 6.** Three different schedules of pipeline parallelism.

We optimize two distributed machine learning workloads using CoCoNET: (i) parameter update using Adam [17], and (ii) point-to-point communication in pipeline parallelism.

**Adam in Data Parallel Training:** Figure 5a shows the traditional implementation of parameter update using Adam. Since each rank has different values of gradients, all ranks obtains the average of these gradients using AllReduce and then perform computations to update optimizer state and the model parameters. Figure 5b presents a schedule that optimizes this parameter update by distributing the pointwise computation on all ranks using a single kernel. The fuse transformation fuses all computations in fusedComp (line 1). Then AllReduce is split into ReduceScatter and AllGather (line 2), such that the computations take output of AllGather (agG) as input. Line 3 reorders AllGather with the computations, such that, each rank performs computations on a slice of the tensors. AllGather operations are returned for parameters and optimizer state. Line 5 slices optimizer states on all ranks to decrease memory usage and removes corresponding AllGather operations. Finally, both communication and computation are fused in a single kernel (line 7).

### Point-to-Point Communication in Pipeline Parallelism:

Figure 6a shows the implementation of pipeline parallelism in Megatron-LM. Assume that there are two transformer layers with two groups of consecutive ranks with two ranks in each group. Rank  $i$  in group  $j$  is shown by tuple  $(j, i)$  in Figure 6. The first transformer layer is assigned to the first group, such that it uses model parallelism within the transformer layer. The next transformer layer is assigned to the second group. First, all ranks in the first group reduces their input ( $in$ ) using AllReduce to get replicated output. Each rank in the first group sends the output to the corresponding rank in the second group using point-to-point

```

1 Var sum = AllReduce("+", in);
2 Var recv = Send(sum, GroupRank(GROUP+1, RANK));
3 Var dropout = Dropout(recv+b,0.1);
4 Var output = dropout + r;
5
6 Execute transformer({in}, {output});

```

(a) Traditional implementation with each rank of a group sending redundant data to next group.

```

1 fuseOut = fuse(recv, dropout, output);
2 fuseSend = fuseComm(recv, fuseOut);
3 (rsSum, agSum) = split(sum, AllReduceSplitRSAG);
4 (scSend, agOut) = reorder(fuseSend, agSum,
5 AllGatherReorder);
6 overlapOut = overlap(rsSum, scSend, agOut);

```

(b) An Optimized Schedule. Each rank sends only a slice of data to ranks in next group and all operations are overlapped.

**Figure 7.** Optimizing pipeline parallelism of Megatron-LM. Input tensors: layer output  $in$ , bias  $b$ , and residual  $r$ .

(P2P) sends, over which several pointwise computations are done (Figure 6 omits the computation for simplicity but they are discussed in Figure 7). Because the output of AllReduce in Figure 6a is replicated, same values are send using P2P. This unnecessary communication is costly because each group is a node in cluster and inter-node links used for P2P are slower than intra-node. Figure 6b shows how this can be optimized using CoCoNET by splitting the AllReduce to ReduceScatter and AllGather and reordering the P2Ps with the AllGather operation. Hence, the inter group communication is reduced by the group size which is 2 in this example. This communication pattern can be further optimized by overlapping the communication operations in Figure 6b. Figure 6c shows that if the buffers are split into multiple tiles ( $T_0$ – $T_2$  in the figure), intra-group and inter-group communications can be overlapped to further reduce the communication time.

Figure 7 shows how to enable the aforementioned optimizations with CoCoNET. Note that in here the computations in Lines 3 and 4 are performed after the P2P communications which were omitted from Figure 6. Figure 7a is the original program, while Figure 7b optimizes by applying the transformations. Lines 1–2 fuses the P2P send with computations. At Line 3 AllReduce is split and the returned AllGather is reordered with fused send at Line 5 so that both P2P send and computations are performed on only a slice of data on the second group where the AllGather is also performed. Finally, all three new operations get overlapped in Line 6. Note that overlapping can only be achieved by generating custom communication and computation kernels.

## 5 CoCoNET Implementation

CoCoNET generates both device code and host code for a CoCoNET program. The host code is generated by traversing the program DFG in a topological order to add kernel calls for each operation. For pointwise computations that are not

part of a communication primitive, CoCoNET generates a stand-alone CUDA kernel. All other codegen falls into one of the categories below: i) a call to a communication collective; ii) a custom kernel that extends a communication collective with a fused-collective (Section 5.3); and iii) a custom kernel that extends a communication collective with overlapping of communication and computation kernels (Section 5.4).

The following sections discuss how CoCoNET adapts NCCL, a widely-used hand-optimized high performance communication library, into a runtime that can execute ii) and iii) above. NCCL is designed for single buffer tensors and is not built to execute arbitrary computations.

### 5.1 NCCL Architecture

NCCL’s architecture defines three key properties: (i) topology, (ii) protocols, (iii) channels, and (iv) threads in a thread block of the CUDA kernel. NCCL automatically sets key architectural properties values based on the size of input buffer, network architecture, and size of WORLD. To get good performance, CoCoNET’s codegen must balance their trade-offs when extending NCCL to custom computation. We now provide a high level overview of these architectural properties.

**Topology** NCCL has two possible communication patterns, a ring and a tree.

**Channels** NCCL maps copies of a topology (ring or tree) to the interconnect network on which it runs. Each copy is called a channel and is assigned to one CUDA thread block. To increase parallelism, more channels are used as the buffer size grows.

**Protocols** NCCL sends data using one of three protocols: LL, LL128, and Simple. These protocols make different tradeoffs between latency and bandwidth, with LL having the lowest latency and Simple having the highest bandwidth.

**Number of Threads** NCCL sets a fixed number of threads for each channel (and thread block). NCCL’s kernels have high register usage, which in practice limits the number of thread blocks per SM to one.

**CoCoNET + NCCL** CoCoNET modifies NCCL so it can do custom computation and overlap other kernels with communication. After determining the topology, protocol, number of channels, and number of threads, NCCL calls the CUDA kernel for the collective. Figure 9 shows the operation of a CoCoNET modified AllReduce NCCL kernel. Each collective communication has three levels of tiling due to the fine-grained parallelism of GPUs. Data is first divided into *buffer tiles* equal to the size of the communication buffer. Each buffer tile is further divided among all ranks and channels to obtain *chunks*. Each channel communicates a chunk of data at a time. The *threads* in channels copy elements in and out of the communication buffers and apply reduction operations (sum, min, max) if needed. The following sections goes into more detail about CoCoNET’s codegen.

## 5.2 CodeGen for Scattered Tensor Communications

In data parallelism, communication and computation occur on different layers of widely different sizes. Existing machine learning frameworks allocate parameters and gradients of layers in non-contiguous buffers, which means that gradients should be copied to larger contiguous buffers to avoid launching too many AllReduce operations.

CoCoNET supports generating a single kernel for operations acting on a list of non-contiguous tensors. The code generation involved is non-trivial because NCCL’s code makes many assumptions of buffers being contiguous. Since each thread of a NCCL channel copies only a few elements in each iteration, indexing the correct tensor at the correct offset could have significant overhead. In a naive implementation each thread would do a binary search in the list of tensors to find the correct one for its index.

CoCoNET avoids this overhead by first dividing each tensor into buckets of size at most 1024 elements and then assigns buckets to warps in a round-robin manner. This mechanism allows each thread to quickly find the offset in a tensor since a warp can directly index in its assigned bucket without having to search. The extra arithmetic involved can add significant overhead and thus CoCoNET pre-calculates the number of buckets that belong to the same contiguous buffer and calculates the offset for all of them once.

The process of breaking each tensor to buckets has some compute and memory overhead. Since this bucketing is done only once on the CPU and training tasks run for thousands of iterations on the same tensors, the computation overhead is negligible and far less than flattening and unflattening in the application. For each bucket, CoCoNET packs an 8-byte tensor address and a 4-byte bucket offset into the associated tensor. This requires  $(8 + 4) \times \lceil \frac{N}{1024} \rceil$  bytes of memory, where  $N$  is the number of elements in a tensor. This memory overhead is negligible as usually only about 0.3% ~ 0.6% the size of the tensors themselves.

## 5.3 CodeGen for Fused Collective

CoCoNET further extends the code generation described in the previous sections to support fused communication collectives. To achieve this, CoCoNET extends NCCL to allow for arbitrary pointwise computations and reductions (i.e., beyond min, max, and sum). We inspected more than 10K lines of code in NCCL to identify where computations can be added so that intermediate values from communication primitives can be directly passed to the computation through registers. CoCoNET supports fusion of both pointwise operations and reductions into NCCL collectives.

Each NCCL protocol utilizes a different mechanisms for communication and CoCoNET generates code for all of them. The important features of a protocol are the pack type (64-bit for LL, 128-bit for LL128 and Simple) and the load/store access patterns (shared memory for LL128, global memory

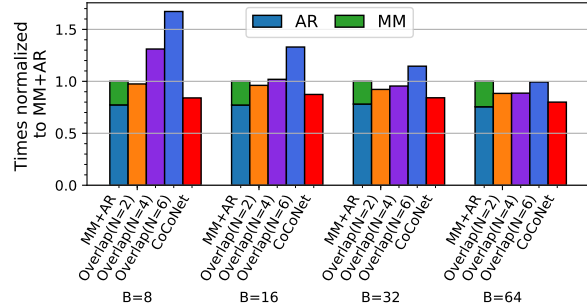


**Figure 8.** Comparison of traditional overlapping and CoCoNET’s overlapping over MatMul and AllReduce (MM+AR) of parallel Self-Attention in GPT-2 on DGX-2 with 16 Tesla V100. (input tensor size: [B, 1024, 192], weights size: [192, 3072], B: batch-size.) MM+AR is sequential; Overlap(N=x) denotes traditional overlapping with x pipeline phases.

for LL and Simple). CoCoNET generates templates for all element types in NCCL, and dispatches accordingly at runtime. There are some subtleties in the code generation process worth discussing:

**Mixed Precision** When the element types of computations and the input tensors are different, CoCoNET finds the largest element type and based on the pack type of the protocol calculates how many elements can be loaded at once. All code will then be generated to operate on this many elements.

**Sliced Tensor** When a sliced tensor is used by a fused communication collective, accesses performed for each channel need to be mapped to elements of the sliced tensor. CoCoNET generates code that produces this mapping. For AllGather the inverse mapping is also produced.

**Tensor Reduction** When reducing a sliced tensor each rank first reduces locally, followed by an AllReduce. The additional AllReduce reuses connections already established between ranks in the surrounding collective kernel, eliminating extra startup latency.

## 5.4 Overlapping of Communication and Computation in CoCoNET

A traditional approach of overlapping computation with its following communication is to divide the data into  $N$  parts and execute a pipeline of  $N + 1$  phases. For each phase  $i$ , *computation* kernel is invoked on the  $i$ th part (except in the last phase) and *communication* kernel is invoked on the  $(i - 1)$ th part (except in the first phase). Both kernels are overlapped by executing concurrently them on different streams. The “Overlap” bars in Figure 8 show the performance of this approach decreases when increasing the number of pipeline phases  $N$ . Performance drops for two reasons: (i) decreasing data size per phase reduces achieved communication bandwidth, and (ii) set-up communication costs increases with an increased number of kernel invocations.

CoCoNET addresses this issue with a mixture of *fine-grained* and *coarse-grained* pipelining. CoCoNET’s generated code invokes the compute and communication kernels on different streams and ensures the producer-consumer relationship between both kernels using a fine-grained spin-lock on a memory buffer as synchronization.

Figure 9 shows an example of overlapping computation and AllReduce for 128 MB of data with 64 MB communication buffer and 8 MB chunk size. In a ring-based AllReduce, each rank communicates chunks based on its position in the ring, which leads to different pipeline phases for each rank. In the example, rank 0 has two fine-grained phases while rank 1 has three.

Both ranks invoke the compute kernel at  $T=①$  on  $M$  different chunks, where  $M$  defines the minimum granularity of fine-grained pipelining. Here we set  $M$  to 2, which splits each coarse-grained phase of eight chunks into fine-grained phases of four chunks. The host waits for the computation to finish at  $T=②$  and invokes the AllReduce kernel to communicate the first four chunks. In parallel, the computation kernels on both ranks compute next four chunks.

On rank 0 all chunks are in a contiguous order and thus the computation for the next four chunks can proceed in a single fine-grained phase. At  $T=③$ , the compute kernel finishes the second fine-grained phase and wakes up the AllReduce kernel to start communication at  $T=⑤$ .

On rank 1 not all chunks are in a contiguous order and the second set of chunks is split into two fine-grained phases (2 and 3), where each works on two chunks. At  $T=③$ , the compute kernel for the second fine-grained phase finishes and wakes up the waiting AllReduce kernel, which starts communication at  $T=⑥$  for rank 1. Meanwhile, computation for the fine-grained phase continues and ends at  $T=④$ .

This process allows the computation and communication of the first buffer tile to be overlapped in a fine-grained manner, which reduces the startup latency of AllReduce. Choosing a value for  $M$  involves a tradeoff between startup latency and parallelism. A smaller  $M$  allows the AllReduce to start earlier, while a larger  $M$  may improve the performance of the computation kernels in the fine-grained phase.

For subsequent buffer tiles, CoCoNET’s generated code follows a coarse-grained pipelining, starting with computation at  $T=④$  on rank 0 and  $T=⑤$  on rank 1. The AllReduce kernel is woken up when the computation finishes (at  $T=⑦$  for rank 0 and  $T=⑧$  for rank 1). The pipeline ends after the last buffer tile is communicated.

Figure 8 shows that the combination of fine-grained and coarse-grained pipelining provides up to 24% better performance than the traditional approach and hides a significant amount of computation time.

## 6 Evaluation

We implemented CoCoNET compiler on top of NCCL [29]. In this section, we demonstrate the effectiveness of CoCoNET by evaluating it on both micro-benchmarks as well as end-to-end distributed deep learning workloads using data parallelism, model parallelism and pipeline parallelism.

Our experiments are performed on a cluster of NVIDIA DGX-2 nodes where each node contains 16 NVIDIA Tesla V100 (32GB) GPUs. Each GPU device within a node is connected to 6 NVSwitches with 6 NVLinks (25GBps for each NVLink). Each node is equipped with dual 24-core (Intel Xeon Platinum 8168) CPUs and 8 non-blocking EDR InfiniBand (100Gbps) network adapters. All nodes are installed with Ubuntu 18.04, CUDA 10.2, cuDNN 7.5 and PyTorch 1.5.

### 6.1 Data Parallel Training

**6.1.1 Microbenchmark of Optimizers.** In data parallelism, communication is to get average gradients among ranks, which is then used by the optimizer to update the model parameters. We take 2 widely used optimizers, Adam and LAMB, as examples to evaluate the performance of CoCoNET on distributed parameters update over baselines.

We evaluate with input tensors ranging from  $2^{10}$  to  $2^{30}$  elements. We test implementations with different configurations, including all NCCL protocols, different number of channels, ranging from 2 to Tesla V100’s maximum, i.e., 80. For each tensor setting, we explore all configurations above and shows the best average result over 1000 iterations.

**Baselines** We use implementations of Adam and LAMB from the NVIDIA Apex Library [28], which fuses all computations into a single kernel. However, the computation and communication are separate kernels. Therefore, for distributed parameters update, it first performs an AllReduce over gradients and then call FusedAdam or FusedLAMB to update. We let **AR-FA** and **AR-FL** denote them, respectively.

**CoCoNET Implementations of Optimizers** We obtained following three schedules of Adam and LAMB by applying different CoCoNET transformations:

1. **AR-Adam** and **AR-LAMB** refer to the traditional parameter update technique, i.e., an AllReduce over gradients and then each GPU individually updates all parameters. These schedules fuse all pointwise computations into a single kernel similar to FusedAdam and FusedLAMB. Both schedules are written in 10 lines of code (LoC), while FusedLAMB and FusedAdam in Apex are written in 6.2K LoC.
2. **RS-Adam-AG** and **RS-LAMB-AG** are generated from AR-Adam and AR-LAMB by first splitting the AllReduce into ReduceScatter and AllGather, and then reordering AllGather with the fused computations. Hence, these schedules distribute parameter update computations across all ranks. RS-Adam-AG schedules written in 13 LoC uses same technique as ZeRO [31], which is written in 3K LoC.



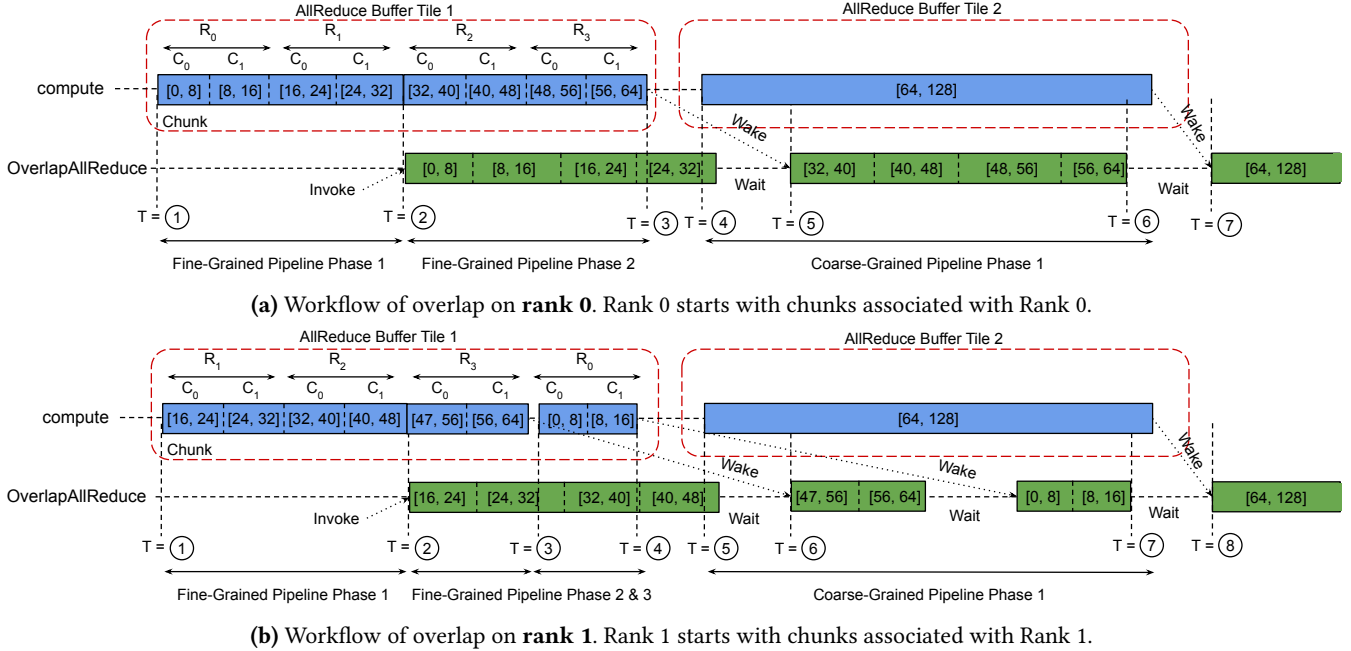


**Figure 9.** Workflow of CoCoNET’s overlapping of producer computation stage with a consumer AllReduce stage for data of size 128MB on 4 ranks ( $R_0$  to  $R_3$ ) with 2 channels ( $C_0$  to  $C_1$ ) and 64 MB buffer size. Size of each chunk is 8MB. CoCoNET’s custom communication kernel allows better overlapping without any decrease in communication bandwidth.

Furthermore, ZeRO does not have a LAMB version, while RS-LAMB-AG is described in only 15 LoC. These schedules can also be represented using GShard [20].

3. **fuse(RS-Adam-AG)** and **fuse(RS-LAMB-AG)** are generated by fusing all stages of RS-Adam-AG and RS-LAMB-AG into FusedAllReduce.

**6.1.2 Results.** We presents results for the following two scenarios: a single contiguous tensor and several non-contiguous tensors.

**Single Tensor** Figure 10 shows the speedup of Adam and LAMB optimizers’ implementations over baseline for different tensor sizes on 64 GPUs (4 DGX-2 nodes). The AllReduce time (without any computation) is the lower bound for execution time of any schedules. We only show results of data type FP16/FP32 mixed-precision as CoCoNET can conveniently change from mixed-precision to FP32 Adam/LAMB implementations and our results are qualitatively similar.

Results show that at least one schedule of CoCoNET is competitive or faster than the baseline AR-FA/AR-FL for all tensors. For Adam optimizer (Figure 10a), speedup of CoCoNET over the AR-FA ranges from 1.2× to 1.7×. For tensors with more than  $2^{19}$  elements, fuse(RS-Adam-AG) provides the best performance since it distributes computations among all GPUs, which reduces computation time. Although RS-Adam-AG also benefits from this, it is still significantly slower than fuse(RS-Adam-AG) till  $2^{28}$  elements because RS-Adam-AG

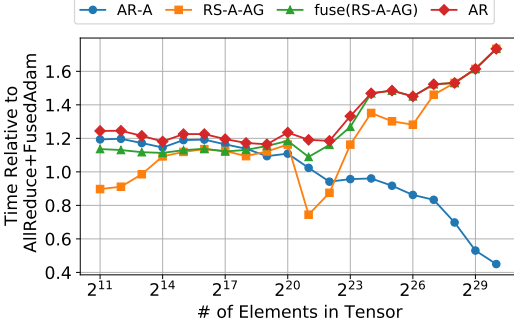
requires two communication collectives, adding extra communication setup latency and performs more global memory accesses. Finally, due to this distribution of computation the time of both fuse(RS-Adam-AG) and RS-Adam-AG approaches the performance of AllReduce.

For LAMB optimizer in Figure 10b, CoCoNET’s best schedule’s speedups ranges from 1.2× to 1.82×. Note that LAMB optimizer requires more computation than Adam optimizer. This explains why the speedup of the best schedule of CoCoNET over the baseline (AR-FL) is higher than Adam’s case (more computation is distributed) and the gap between the AllReduce performance and the best schedule.

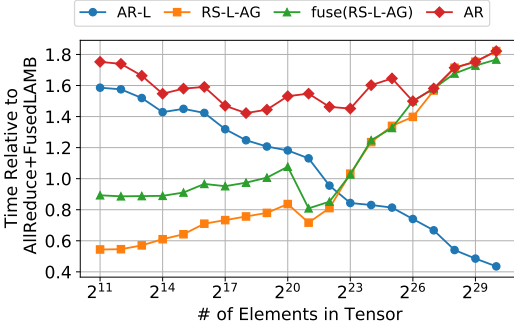
Figure 10 shows that AR-A and AR-L are faster for smaller tensors because communication kernels have a large overhead and the distributed computation do not justify for multiple kernel calls. However, as the tensors gets larger, the distributed computation makes up for the extra latencies.

In summary, CoCoNET provides performance improvements over baselines with less lines of code. Furthermore, there is no transformation that performs the best for all sizes. And for a model, CoCoNET can provide different schedules for different tensors accordingly to achieve its best speedup.

**Scattered Tensors** We discussed in the single contiguous scenario that the overhead of communication kernels is high for small tensors. Therefore, calling a kernel for every single tensor in a model has an excessive amount of overhead. For example, BERT [9] has 360 tensors with elements from 1K



(a) Mixed-precision Adam. *AR-A* refers to AR-Adam, *RS-A-AG* refers to RS-Adam-AG, *fuse(RS-A-AG)* refers to fuse(RS-A-AG), and *AR* refers to only AllReduce.



(b) Mixed-precision LAMB. *AR-L* refers to AR-LAMB, *RS-L-AG* refers to RS-LAMB-AG, *fuse(RS-L-AG)* refers to fuse(RS-LAMB-AG), and *AR* refers to only AllReduce.

**Figure 10.** Speedup of different schedules over baselines on 64 GPUs. (higher is better).

Optimizer	Type	Single Tensor	Scattered Tensor
Adam	FP32	652.77 ms	665.83 ms
	Mixed Precision	333.74 ms	364.29 ms
LAMB	FP32	692.44 ms	697.75 ms
	Mixed Precision	366.05 ms	360.84 ms

**Table 1.** Execution time of CoCoNET scattered tensors and single buffer fuse(RS-Optimizer-AG) transformation. (BERT layer tensor sizes, 64 GPUs, 20 iterations)

to 31M. Table 1 compares the performance of Adam/LAMB optimizers with FP32 or mixed precision on 64 GPUs with 360 tensor sizes from the BERT model against a single contiguous tensor with the size equal to the summation of BERT model tensors which is 340 million elements. All variants use fuse(RS-Optim-AG) as it has the best performance at this size. As the numbers suggest, CoCoNET generated scattered tensors code is competitive with the single buffer code and any overhead will be made up by avoiding multiple kernel launches or copies of data into a single buffer.

**6.1.3 Integration with BERT.** We evaluate the integration of CoCoNET generated optimizers to the BERT model from NVIDIA [26]. We use the BERT-Large configuration

and train using the Adam optimizer with mixed precision and an 8k global batch size.

**BERT baseline** To avoid invoking AllReduce for each layer separately, the original model script allocates a single buffer that can hold gradients for all model parameters. After each backward pass, it uses Apex [28] to copy all gradients into the buffer and then calls AllReduce on the buffer. After AllReduce the model script again uses Apex to copy the gradients back to their original tensors and calls Apex’s FusedAdam.

**BERT with CoCoNET** We replace the procedure of AllReduce and optimizer in the baseline with a single call to *fuse(RS-Adam-AG)*. CoCoNET’s scattered tensors support eliminates copying data to and from a contiguous buffer.

**Potential Speedup** To see how much speedup we could expect, we produced a timing breakdown of an iteration of the baseline:

GPU#	Time(s)	Copies	AllReduce	Adam	Potential
16	2.37	0.4%	0.3%	0.7%	1.1%
32	1.44	0.6%	1.2%	1.1%	1.7%
64	0.64	1.3%	2.9%	2.5%	3.8%

The parts CoCoNET can improve are “Copies” and the portion of “Adam” that can be distributed and hidden into “AllReduce”. The “Potential” column gives the maximum potential speedup. Strong scaling improves the gradient computation time but the optimizer and the AllReduce do not get faster. Therefore, potential speedup goes up with more GPUs as long as strong scaling holds up. BERT model can be trained with up to 2048 GPUs [1]. For our largest setup of 64 GPUs the maximum speedup we could get is 3.8%.

**Actual Speedup** We used 64 V100 GPUs across 4 DGX2 nodes to train BERT and measure the iteration time. We measured speedup from 100 samples gathered after a sufficient warmup to stabilize the iteration time and report the speedup as an average over 10 executions.

BERT with CoCoNET offers an average speedup over the baseline of 3.5%, which is closer to the potential speedup.

**Memory Savings** We evaluated the memory savings from (1) only allocating a slice of the optimizer state on each GPU and (2) not having to allocate large contiguous buffers to copy gradients into. When using a maximum sequence length of 128 tokens, the maximum batch size that the baseline can fit in memory is 76 samples. Meanwhile, using *fuse(RS-Adam-AG)* allows a maximum batch size of 86 samples. Since PyTorch DDP does not slice optimizer state updates, it also has maximum batch size of 76 samples. Having a larger model or less available memory would make the improvement even larger [31]. Any advantage from this larger batch size is not included in the speedups above, as the BERT training script assumes a power-of-two batch size.

## 6.2 Model Parallelism

Megatron-LM [34] uses a model parallel approach for efficient inference and training for transformer based language models, such as BERT [9] and GPT [5]. A transformer layer contains two blocks, a self-attention block, and a multi-layer perceptron (MLP) block. A self-attention block contains different operations but the last few ones are the same computations as shown in Figure 2. An MLP block’s last operations are similar to Figure 2 except that the input tensor and weight sizes are  $[B, S, 4 \times H]$  and  $[4 \times H, H]$ .  $B$ ,  $S$  and  $H$  are batch size, sequence length and hidden size, respectively. We implemented both computations in CoCoNET and obtained three schedules by applying one or more transformations:

1. **MM+AR+C** refers to the traditional model parallelism technique described in Figure 2. This schedule fuses all pointwise computations into a single kernel.
2. **MM+RS+C+AG** is generated from MM+AR+C by splitting AllReduce into ReduceScatter and AllGather, and then reordering AllGather and computations. This schedule is similar to the schedule that will be generated by GShard [20] after sharding the output of matrix multiplication across all ranks.
3. **O(MM,fuse(RS+C+AG))** is generated from previous schedule by fusing the ReduceScatter, computation, and AllGather into a FusedAllReduce and then overlapping it with matrix multiplication.

**Results** We evaluate these schedules with a GPT-2 8.3 Billion parameter model (i.e.,  $S = 1024$ ,  $H = 3072$ ) on one DGX-2 node with 16 GPUs. We evaluate for batch sizes ( $B$ ) from 8 to 64. Figure 11 shows the times of all schedules normalized to time of MM+AR+C and the breakdown of time spent in communication and computation. MM+RS+C+AG provides  $1.05\times$  to  $1.17\times$  speedup over MM+AR+C by distributing computations on all ranks, even though MM+RS+C+AG spends longer in communication due to the latency of two communication collectives (ReduceScatter and AllGather) instead of a single AllReduce. O(MM,fuse(RS+C+AG)) provides  $1.2\times$  to  $1.33\times$  speedup over MM+AR+C and  $1.07\times$  to  $1.2\times$  over MM+RS+C+AG. O(MM,fuse(RS+C+AG)) improves over both schedules by using FusedAllReduce, distributing computation, and overlapping it with the matrix multiplication.

**6.2.1 Integration with Megatron-LM.** We evaluated inference times of GPT-2 8.3 Billion parameter model after integrating both MM+RS+C+AG (similar to GShard) and O(MM,fuse(RS+C+AG)) schedules in Megatron-LM [34]. The table below shows the speedups over the baseline Megatron-LM implementation for batch size 8 on 8 and 16 GPUs,

GPU#	MM+RS+C+AG	O(MM,fuse(RS+C+AG))
8	1.14×	1.23×
16	1.2×	1.4×

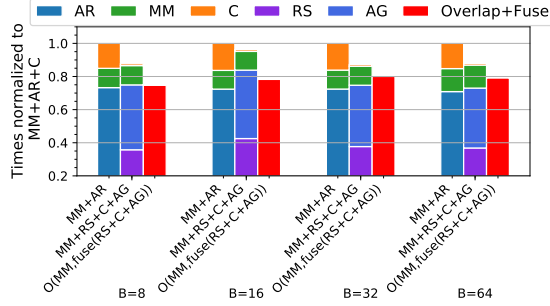
Overlapping matrix multiplication with AllReduce and pointwise computations (performed by FusedAllReduce) significantly improves inference times in GPT-2. Speedups are larger than mentioned in Figure 11 because unlike the schedules Megatron-LM does not fuse the pointwise computations.

## 6.3 Pipeline Parallelism

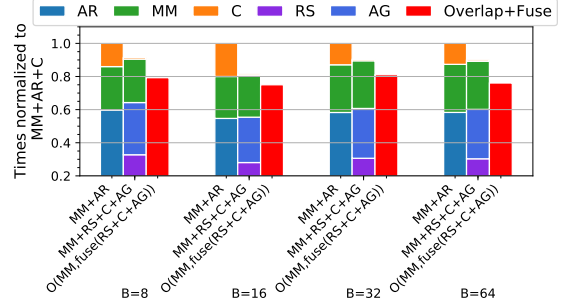
CoCoNET can optimize inference in pipeline parallelism by overlapping different communication operations as discussed in Section 4 in Figures 6 and 7. We evaluated CoCoNET on computations of model and pipeline parallelism in Megatron-LM over GPT-3 175B model. A transformer layer contains several operations but the operations of interest for this experiment are presented in Figure 7a. To show the diverse code generation supported by CoCoNET, we performed evaluation on a cluster of 16 nodes where cross node communication happens with 8 InfiniBand network adapters (200Gbps each) and each node contains 8 NVIDIA Tesla A100 GPUs (40GB for each) connected by 6 NVSwitches and 12 NVLinks (25GBps for each NVLink). We evaluated following:

1. **AR+P2P+C** refers to the original Megatron-LM design of model and pipeline parallelism described in Figure 7a.
2. **AR+P2P+C+AG** is generated from AR+P2P+C by slicing the output of AllReduce, performing both P2P sends and compute on the sliced output, and AllGather to obtain final output. This is similar to Narayanan et al. [25] idea where schedule AR+P2P+AG+C was used and the output of AllReduce was sliced to reduce the communication volume. However, the computation is still replicated since it happens after the AllGather.
3. **RS+P2P+C+AG** is generated by splitting AllReduce into ReduceScatter and AllGather, then reordering AllGather with the P2P send and computation, hence, removing redundant computation and communication. This schedule is similar to the schedule that will be generated by GShard [20] after sharding the input of AllReduce.
4. **O(RS+C,P2P,AG)** is generated from RS+P2P+C+AG by first fusing computation with ReduceScatter, and then overlapping all three communication operations. Figure 6c shows how overlapping is performed.

**Results** Figure 12 shows the breakdown of the computation/communication in Figure 7 on two nodes of our A100 cluster where each node contains a transformer layer. The sequence length ( $S = 2048$ ) and the hidden size ( $H = 12288$ ) are set based on GPT-3 175 billion parameter model. O(RS+C,P2P,AG) is  $11.38\times$  faster than AR+P2P+C,  $3\times$  over AR+P2P+C+AG,  $2.14\times$  faster than RS+P2P+C+AG schedule. The speedups come from three sources: (i) smaller P2Ps reduces cross node communication volume, (ii) fusing all communication and computation kernels into one reduces memory accesses and allows better network and GPU memory bandwidth utilization, and (iii) communication in different connections



(a) Model Parallel Self-Attention with input size  $[B, S, H \div 16]$  and weights of size  $[H \div 16, H]$ .



(b) Model Parallel Multi-Layer Perceptron with input size  $[B, S, 4 \times H \div 16]$  and weights of size  $[4 \times H \div 16, H]$ .

**Figure 11.** Times of three schedules of model parallel self-attention and multi-layer perceptron of GPT-2 in CoCoNET normalized to the baseline schedule, i.e., MM+AR+C for two matrix multiplication sizes for 16 Tesla V100 GPUs. Breakdown of time spent in different kernel calls is shown for MM+AR and MM+RS+C+AG.

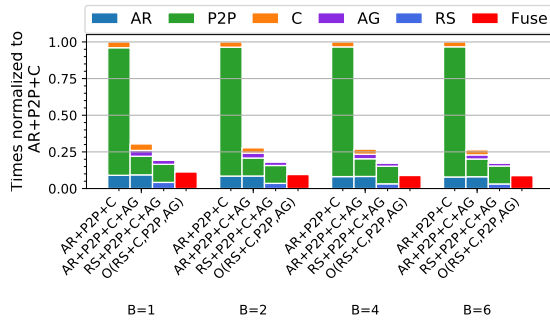


**Figure 12.** Times of four schedules of forward pass per batch for GPT-3 175B model in CoCoNET normalized to the baseline schedule, i.e. AR+P2P+C, applying pipeline parallelism across nodes and model parallelism within node.

(NVLink within node and InfiniBand across nodes) overlapped with each other to provide better utilization of network bandwidth, while other schedules can utilize only one stack at a time.

**Integration with Megatron-LM** We evaluated forward time of models with multiple transformer layers on 16 A100 nodes. The first experiment has one transformer layer per node (a total of 16 layers) and the second one has 6 transformers per layer (a total of 96 layers). The second setup is GPT-3 175 billion parameters. Ideally in a large scale inferecing, GPT-3 175 billion parameters is executed on 96 nodes so that each node has one transformer per node. To replicate this scenario, we designed the first experiment to show our speed up numbers in larger scale.

In the first experiment, our  $O(RS+C+,P2P,AG)$  schedule in Megatron-LM is  $2.03\times$  faster than the original implementation. This shows how much speed up we can expect with 96 nodes running GPT-3 175 billion parameter model. For the second experiment, our  $O(RS+C+,P2P,AG)$  schedule in Megatron-LM is  $1.19\times$  faster than the original implementation which is for the true GPT-3 175 billion parameter model. This shows how significant CoCoNET can improve the performance of Megatron-LM.

## 7 Related Work

**Optimizing Stencil Computations** Several domain specific languages have been proposed to optimize data-parallel stencil computations on CPUs, GPUs, and other accelerators. Halide [30] and Fireiron [12] separate the algorithm and schedule, which describes the optimizations like fusion, and loop tiling. LIFT [13, 35] includes a functional language and optimizes stencil computations by applying rewrite rules. None of these works support distributed systems.

Distributed-Halide [8] extends Halide with scheduling primitives that allow distributing parallelizable dimensions of loops. It will then generate MPI sends and receives for the necessary communication on boundaries of slices. CoCoNET extends this work to explicitly reason about and compose communication collectives with computation, which is crucial for distributed machine learning scenarios.

**Overlapping Computation and Communication** Existing works [2, 18, 22, 23, 36] uses either pipelined execution to overlap communication and computation or non-blocking operations. Pencil [37] improves upon these works by performing pipelining within a process and supports computations in multiple connected iteration spaces. Several techniques distribute tiles and automatically generate communication [4, 8, 32]. Basu et. al. [3] uses overlapped tiling in each process to remove communication between processes. Denis and Trahay [7] studied the efficiency of overlap. dCUDA [11] provides hardware supported overlap. These works for MPI+OpenMP are valid for stencil computations that require sends and receives to share the halo regions. However, CoCoNET supports collectives and several transformations that these works do not support.

**Distributed Neural Network Training** Several works have improved data parallel and model parallel techniques. Mesh-Tensorflow [33] and GShard [20] create *shards* of weights and model state that can be split among ranks. ZeRO [31] splits weights and model state among ranks and uses ReduceScatter and AllGather to distribute computation. FlexFlow [15]



performs operator splitting as a way to represent both data-parallelism and model-parallelism, but do not optimize computation with communication. CoCoNET improves on these works by providing a general abstraction that (i) supports computation and communication collectives, (ii) ensure correctness, and (iii) allows the developer to explore several optimizations. CoCoNET also provides several optimizations that are possible only due to the abstraction: (i) scattered tensors that removes extra storage and memory copy operations, (ii) fusion communication collectives, and (iii) novel communication and computation overlapping techniques. PyTorch’s DDP [21] overlaps AllReduce of gradients with the forward and backward pass. However, unlike CoCoNET, PyTorch’s DDP requires extra memory for overlapping, which can increase training time for very large models [27] and do not support slicing of optimizer parameter update that significantly decreases memory usage. GPipe [14], Pipedream [24] and Narayanan et al. [25] proposed pipeline training to improve model parallelism, by dividing the forward and backward pass into several mini-batches, which are then pipelined across devices. CoCoNET improves on these works by overlapping inter and intra-node communication operations.

## 8 Conclusion

This paper introduced CoCoNET: a language to describe and schedule distributed machine learning computations, and a compiler and runtime to execute them. CoCoNET’s transformations allow users to easily explore a space of optimizations for both model and data parallel scenarios. Through a series of experiments, we show CoCoNET generated code is significantly better than hand-optimized baselines. In future we plan to automate the exploration of optimizations through smart search.

## References

- [1] Accessed: 2021-05-05. ML Commons. <https://mlcommons.org/en/>.
- [2] Youcef Barigou and Edgar Gabriel. 2017. Maximizing Communication-Computation Overlap Through Automatic Parallelization and Runtime Tuning of Non-blocking Collective Operations. *International Journal of Parallel Programming* 45, 6 (01 Dec 2017), 1390–1416. <https://doi.org/10.1007/s10766-016-0477-7>
- [3] P. Basu, A. Venkat, M. Hall, S. Williams, B. Van Straalen, and L. Oliker. 2013. Compiler generation and autotuning of communication-avoiding operators for geometric multigrid. In *20th Annual International Conference on High Performance Computing*. 452–461. <https://doi.org/10.1109/HiPC.2013.6799131>
- [4] Uday Bondhugula. 2013. Compiling Affine Loop Nests for Distributed-Memory Parallel Architectures. In *Proceedings of the International Conference on High Performance Computing, Networking, Storage and Analysis* (Denver, Colorado) (SC ’13). Association for Computing Machinery, New York, NY, USA, Article 33, 12 pages. <https://doi.org/10.1145/2503210.2503289>
- [5] Tom B. Brown, Benjamin Mann, Nick Ryder, Melanie Subbiah, Jared Kaplan, Prafulla Dhariwal, Arvind Neelakantan, Pranav Shyam, Girish Sastry, Amanda Askell, Sandhini Agarwal, Ariel Herbert-Voss, Gretchen Krueger, Tom Henighan, Rewon Child, Aditya Ramesh, Daniel M. Ziegler, Jeffrey Wu, Clemens Winter, Christopher Hesse, Mark Chen, Eric Sigler, Mateusz Litwin, Scott Gray, Benjamin Chess, Jack Clark, Christopher Berner, Sam McCandlish, Alec Radford, Ilya Sutskever, and Dario Amodei. 2020. Language Models are Few-Shot Learners. In *Advances in Neural Information Processing Systems*, Vol. 31. <https://proceedings.neurips.cc/paper/2018/file/3a37abdeefe1dab1b30f7c5c7e581b93-Paper.pdf>
- [6] Jeffrey Dean, Greg Corrado, Rajat Monga, Kai Chen, Matthieu Devin, Mark Mao, Marc aurelio Ranzato, Andrew Senior, Paul Tucker, Ke Yang, Quoc Le, and Andrew Ng. 2012. Large Scale Distributed Deep Networks. In *Advances in Neural Information Processing Systems*, F. Pereira, C. J. C. Burges, L. Bottou, and K. Q. Weinberger (Eds.), Vol. 25. Curran Associates, Inc., 1223–1231. <https://proceedings.neurips.cc/paper/2012/file/6aca97005c68f1206823815f66102863-Paper.pdf>
- [7] A. Denis and F. Trahay. 2016. MPI Overlap: Benchmark and Analysis. In *2016 45th International Conference on Parallel Processing (ICPP)*. 258–267. <https://doi.org/10.1109/ICPP.2016.37>
- [8] Tyler Denniston, Shoaib Kamil, and Saman Amarasinghe. 2016. Distributed Halide. In *Proceedings of the 21st ACM SIGPLAN Symposium on Principles and Practice of Parallel Programming* (Barcelona, Spain) (PPoPP ’16). Association for Computing Machinery, New York, NY, USA, Article 5, 12 pages. <https://doi.org/10.1145/2851141.2851157>
- [9] Jacob Devlin, Ming-Wei Chang, Kenton Lee, and Kristina Toutanova. 2019. BERT: Pre-training of Deep Bidirectional Transformers for Language Understanding. arXiv:1810.04805 [cs.CL]
- [10] Message Passing Interface Forum. 2012. MPI: A Message-Passing Interface Standard Version 3.0. Chapter author for Collective Communication, Process Topologies, and One Sided Communications.
- [11] Tobias Gysi, Jeremia Bär, and Torsten Hoefler. 2016. DCUDA: Hardware Supported Overlap of Computation and Communication. In *Proceedings of the International Conference for High Performance Computing, Networking, Storage and Analysis* (Salt Lake City, Utah) (SC ’16). IEEE Press, Article 52, 12 pages.
- [12] Bastian Hagedorn, Archibald Samuel Elliott, Henrik Barthels, Rastislav Bodik, and Vinod Grover. 2020. Fireiron: A Data-Movement-Aware Scheduling Language for GPUs. In *Proceedings of the ACM International Conference on Parallel Architectures and Compilation Techniques* (Virtual Event, GA, USA) (PACT ’20). Association for Computing Machinery, New York, NY, USA, 71–82. <https://doi.org/10.1145/3410463.3414632>
- [13] Bastian Hagedorn, Larisa Stoltzfus, Michel Steuwer, Sergei Gorlatch, and Christophe Dubach. 2018. High Performance Stencil Code Generation with Lift. In *Proceedings of the 2018 International Symposium on Code Generation and Optimization* (Vienna, Austria) (CGO 2018). Association for Computing Machinery, New York, NY, USA, 100–112. <https://doi.org/10.1145/3168824>
- [14] Yanping Huang, Youlong Cheng, Ankur Bapna, Orhan Firat, Dehao Chen, Mia Chen, HyoukJoong Lee, Jiquan Ngiam, Quoc V Le, Yonghui Wu, and zhifeng Chen. 2019. GPipe: Efficient Training of Giant Neural Networks using Pipeline Parallelism. In *Advances in Neural Information Processing Systems* 32, H. Wallach, H. Larochelle, A. Beygelzimer, F. dAlcheBuc, E. Fox, and R. Garnett (Eds.). Curran Associates, Inc., 103–112. <http://papers.nips.cc/paper/8305-gpipe-efficient-training-of-giant-neural-networks-using-pipeline-parallelism.pdf>
- [15] Zhihao Jia, Matei Zaharia, and Alex Aiken. 2019. Beyond Data and Model Parallelism for Deep Neural Networks. In *Proceedings of Machine Learning and Systems*, A. Talwalkar, V. Smith, and M. Zaharia (Eds.), Vol. 1. 1–13. <https://proceedings.mlsys.org/paper/2019/file/c74d97b01eae257e44aa9d5bade97baf-Paper.pdf>

- [16] Marcin Junczys-Dowmunt, Roman Grundkiewicz, Tomasz Dwojak, Hieu Hoang, Kenneth Heafield, Tom Neckermann, Frank Seide, Ulrich Germann, Alham Fikri Aji, Nikolay Bogoychev, André F. T. Martins, and Alexandra Birch. 2018. Marian: Fast Neural Machine Translation in C++. In *Proceedings of ACL 2018, System Demonstrations*. Association for Computational Linguistics, Melbourne, Australia, 116–121. <http://www.aclweb.org/anthology/P18-4020>
- [17] Diederik P. Kingma and Jimmy Ba. 2014. Adam: A Method for Stochastic Optimization. <http://arxiv.org/abs/1412.6980> cite arxiv:1412.6980Comment: Published as a conference paper at the 3rd International Conference for Learning Representations, San Diego, 2015.
- [18] N. Koziris, A. Sotiropoulos, and G. Goumas. 2003. A pipelined schedule to minimize completion time for loop tiling with computation and communication overlapping. *J. Parallel and Distrib. Comput.* 63, 11 (2003), 1138 – 1151. [https://doi.org/10.1016/S0743-7315\(03\)00102-3](https://doi.org/10.1016/S0743-7315(03)00102-3)
- [19] Alex Krizhevsky, Ilya Sutskever, and Geoffrey E Hinton. 2012. ImageNet Classification with Deep Convolutional Neural Networks. In *Advances in Neural Information Processing Systems*, F. Pereira, C. J. C. Burges, L. Bottou, and K. Q. Weinberger (Eds.), Vol. 25. Curran Associates, Inc., 1097–1105. <https://proceedings.neurips.cc/paper/2012/file/c399862d3b9d6b76c8436e924a68c45b-Paper.pdf>
- [20] Dmitry Lepikhin, HyoukJoong Lee, Yuanzhong Xu, Dehao Chen, Orhan Firat, Yanping Huang, Maxim Krikun, Noam Shazeer, and Zhifeng Chen. 2020. GShard: Scaling Giant Models with Conditional Computation and Automatic Sharding. arXiv:2006.16668 [cs.CL]
- [21] Shen Li, Yanli Zhao, Rohan Varma, Omkar Salpekar, Pieter Noordhuis, Teng Li, Adam Paszke, Jeff Smith, Brian Vaughan, Pritam Damania, and Soumith Chintala. 2020. PyTorch Distributed: Experiences on Accelerating Data Parallel Training. *Proc. VLDB Endow.* 13, 12 (Aug. 2020), 3005–3018. <https://doi.org/10.14778/3415478.3415530>
- [22] H. Lu, S. Seo, and P. Balaji. 2015. MPI+ULT: Overlapping Communication and Computation with User-Level Threads. In *2015 IEEE 17th International Conference on High Performance Computing and Communications, 2015 IEEE 7th International Symposium on Cyberspace Safety and Security, and 2015 IEEE 12th International Conference on Embedded Software and Systems*. 444–454. <https://doi.org/10.1109/HPCC-CSS-ICES.2015.82>
- [23] Vladimir Marjanović, Jesús Labarta, Eduard Ayguadé, and Mateo Valero. 2010. Overlapping Communication and Computation by Using a Hybrid MPI/SMPSs Approach. In *Proceedings of the 24th ACM International Conference on Supercomputing (Tsukuba, Ibaraki, Japan) (ICS '10)*. Association for Computing Machinery, New York, NY, USA, 5–16. <https://doi.org/10.1145/1810085.1810091>
- [24] Deepak Narayanan, Aaron Harlap, Amar Phanishayee, Vivek Seshadri, Nikhil R. Devanur, Gregory R. Ganger, Phillip B. Gibbons, and Matei Zaharia. 2019. PipeDream: Generalized Pipeline Parallelism for DNN Training. In *Proceedings of the 27th ACM Symposium on Operating Systems Principles (Huntsville, Ontario, Canada) (SOSP '19)*. Association for Computing Machinery, New York, NY, USA, 1–15. <https://doi.org/10.1145/3341301.3359646>
- [25] Deepak Narayanan, Mohammad Shoeybi, Jared Casper, Patrick LeGresley, Mostofa Patwary, Vijay Korthikanti, Dmitri Vainbrand, Prithvi Kashinkunti, Julie Bernauer, Bryan Catanzaro, Amar Phanishayee, and Matei Zaharia. 2021. Efficient Large-Scale Language Model Training on GPU Clusters. arXiv:2104.04473 [cs.CL]
- [26] NVIDIA. Accessed: 2021-05-01. NVIDIA BERT. <https://github.com/NVIDIA/DeepLearningExamples>.
- [27] NVIDIA. Accessed: 2021-05-01. NVIDIA Megatron-LM. <https://github.com/NVIDIA/Megatron-LM/>.
- [28] NVIDIA. Accessed: 2021-05-05. Apex. <https://github.com/NVIDIA/apex>.
- [29] NVIDIA. Accessed: 2021-05-05. NVIDIA Collective Communication Library. <https://github.com/NVIDIA/nvcl>.
- [30] Jonathan Ragan-Kelley, Connelly Barnes, Andrew Adams, Sylvain Paris, Frédo Durand, and Saman Amarasinghe. 2013. Halide: A Language and Compiler for Optimizing Parallelism, Locality, and Re-computation in Image Processing Pipelines. In *Proceedings of the 34th ACM SIGPLAN Conference on Programming Language Design and Implementation (Seattle, Washington, USA) (PLDI '13)*. Association for Computing Machinery, New York, NY, USA, 519–530. <https://doi.org/10.1145/2491956.2462176>
- [31] Samyam Rajbhandari, Jeff Rasley, Olatunji Ruwase, and Yuxiong He. 2020. ZeRO: Memory Optimizations toward Training Trillion Parameter Models. In *Proceedings of the International Conference for High Performance Computing, Networking, Storage and Analysis (Atlanta, Georgia) (SC '20)*. IEEE Press, Article 20, 16 pages.
- [32] I. Z. Reguly, G. R. Mudalige, and M. B. Giles. 2018. Loop Tiling in Large-Scale Stencil Codes at Run-Time with OPS. *IEEE Transactions on Parallel and Distributed Systems* 29, 4 (2018), 873–886. <https://doi.org/10.1109/TPDS.2017.2778161>
- [33] Noam Shazeer, Youlong Cheng, Niki Parmar, Dustin Tran, Ashish Vaswani, Penporn Koanantakool, Peter Hawkins, HyoukJoong Lee, Mingsheng Hong, Cliff Young, Ryan Sepassi, and Blake Hechtman. 2018. Mesh-TensorFlow: Deep Learning for Supercomputers. In *Advances in Neural Information Processing Systems*, S. Bengio, H. Wallach, H. Larochelle, K. Grauman, N. Cesa-Bianchi, and R. Garnett (Eds.), Vol. 31. Curran Associates, Inc., 10414–10423. <https://proceedings.neurips.cc/paper/2018/file/3a37abdeefe1dab1b30f7c5c7e581b93-Paper.pdf>
- [34] Mohammad Shoeybi, Mostofa Patwary, Raul Puri, Patrick LeGresley, Jared Casper, and Bryan Catanzaro. 2020. Megatron-LM: Training Multi-Billion Parameter Language Models Using Model Parallelism. arXiv:1909.08053 [cs.CL]
- [35] M. Steuwer, T. Rummelg, and C. Dubach. 2017. LIFT: A functional data-parallel IR for high-performance GPU code generation. In *2017 IEEE/ACM International Symposium on Code Generation and Optimization (CGO)*. 74–85. <https://doi.org/10.1109/CGO.2017.7863730>
- [36] Hari Subramoni, Sourav Chakraborty, and Dhabaleswar K. Panda. 2017. Designing Dynamic and Adaptive MPI Point-to-Point Communication Protocols for Efficient Overlap of Computation and Communication. In *High Performance Computing*, Julian M. Kunkel, Rio Yokota, Pavan Balaji, and David Keyes (Eds.). Springer International Publishing, Cham, 334–354.
- [37] Hengjie Wang and Aparna Chandramowlishwaran. 2020. *Pencil: A Pipelined Algorithm for Distributed Stencils*. IEEE Press.
- [38] Yang You, Jing Li, Sashank Reddi, Jonathan Hseu, Sanjiv Kumar, Srinadh Bhojanapalli, Xiaodan Song, James Demmel, Kurt Keutzer, and Cho-Jui Hsieh. 2020. Large Batch Optimization for Deep Learning: Training BERT in 76 minutes. arXiv:1904.00962 [cs.LG]